

# Electric and magnetic field calculation software in transmission lines

Luis Imbachi Guerrero, Fredy Jiménez Rubio, Mario Rodríguez Barrera, Diego Giral-Ramírez

Technological Faculty, Universidad Distrital Francisco Jose de Caldas, Bogotá, Colombia

---

## Article Info

### Article history:

Received Jul 8, 2021

Revised Jun 8, 2022

Accepted Jul 1, 2022

---

### Keywords:

Electric field  
Magnetic field  
Servitude zone  
Simulation tool  
Transmission line

---

## ABSTRACT

There is an interest in the biological effects of exposure to low-frequency electromagnetic fields issued by transmission lines on animals and humans. The fields generated by the lines are relevant for the design and operation of power systems. The study of the electric and magnetic fields in the transmission networks implemented commercial simulators bases on the finite element method. These commercial simulators are characterized by accuracy and high hardware and software requirements. This work presents CEM-LT, a tool that accurately precisely the electric and magnetic field in the transmission lines, with simple and intuitive handling and low processing times, making it ideal for being implemented together with optimization methods. The electric and magnetic field in the servant area for two case studies is analyzed to evaluate the accuracy and processing times. The level of accuracy is characterized by comparing the results with COMSOL obtaining errors of less than 2.4%. The case study with the highest computational requirement achieved a processing time of 3,027 seconds.

*This is an open access article under the [CC BY-SA](#) license.*



---

## Corresponding Author:

Diego Giral-Ramírez

Technological Faculty, Universidad Distrital Francisco José de Caldas

Street 68 D Bis A Sur # 49 F - 70, Bogotá, Colombia

Email: dagiralr@udistrital.edu.co

---

## 1. INTRODUCTION

This document aims to present software to reduce the high hardware and software requirements directly used by commercial simulators to calculate the electric and magnetic fields based on the finite element method. The implemented software is a computational tool developed in the MATLAB app designer, which only requires a free compiler to calculate the electric field and magnetic field in transmission lines. The CEM-LT software presents acceptable results compared to simulation software based on the finite element method such as COMSOL Multiphysics and its low computational time. Additionally, it represents clean and intuitive handling that does not require long hours of training. Given its most relevant characteristics, such as its low computational time and acceptable accuracy, it is ideal to be implemented in conjunction with stochastic optimization methods such as the particle swarm optimization (PSO). This implementation helps to determine the optimal location of transmission line conductors to minimize the electric field or the transmission lines to minimize the electric field or magnetic field in the easement zone [1], [2].

The transmission of alternating current electrical power [3], generates associated effects such as losses due to the corona effect, audible noise, and radio and television interference. Transmission lines are considered one of the principal sources of electric and magnetic fields [4]–[7]. The intensity of the fields emitted by these lines depends mainly on the transmitted current and their voltages. In the last two decades, there has been a scientific and social interest focused on the risk of the low-frequency electromagnetic fields low frequency electromagnetic field (LF-EMF) emitted by the lines of electrical transmission, considering

the biological effects in animals and humans. The International Agency for Research on Cancer (IRAC) in 2002 classified low-frequency magnetic fields as possible carcinogens for humans (Group 2B) [8]–[12]. The existing scientific evidence does not conclude that prolonged exposure to low-frequency magnetic fields is a cause of childhood leukemia [13]–[16]. However, more studies are required to explore the negative impact on neurobehavioral function in children due to LF-EMF exposure [17]–[19]. The research has not shown to date that prolonged exposure to Low levels of LF-EMF has detrimental effects on health [20], [21].

The International Commission for the Protection of Non-Ionizing Radiation (ICNIRP) specifies within its guidelines [22], the reference levels, understood as the levels of the electric and magnetic field in an efficient value, to which a person can be exposed without adverse effects and with an adequate safety factor. In particular, for a frequency of 60 Hz and occupational exposure, the reference values for electric field intensity and magnetic flux density correspond to 8.3 kV/m and 1 mT. In the same way, for the general public, the reference values for electric field intensity and magnetic flux density correspond to 4.16 kV/m and 0.2 mT. The electric and magnetic fields generated by transmission lines play a meaningful role in the design and operation of electrical networks; in this way, it establishes some procedures for their measurement [23]. In the easement zone or the right-of-way permit along the transmission line, the electric and magnetic field values must be lower than the reference levels specified above. If the rates of the fields are above the permissible limits, the design should be revised [4], [24].

Through a documentary review on electric and magnetic fields in transmission lines, multiple works associated with software development with an interface that eases the learning process, or the accompaniment as a work tool, were identified. Thus, in study [4], the authors analyze the design of a 765 kV line in Gujarat, India. In this study, they determine the field profiles employing an interface developed in the MATLAB Guide application. Similarly, in [25], a study performed an analysis of electric and magnetic fields generated by two transmission lines (single and double circuit) of 400 kV in Romania, so the developers evaluate the field profiles in a program written in LabVIEW. Additionally, in [26], software developed in the MATLAB guide application is created, which calculates the fields generated by multi-circuit transmission lines, providing 2D and 3D field profiles. It evidenced that when comparing the field profiles of a 230 kV line in Brazil with a study conducted by the São Francisco Hydroelectric Company (CHESF).

Without developing any interface software, Unde and Kushare [27] carried out an analysis with MATLAB of the electric and magnetic field in a 1,200 kV transmission line installed in Madhya Pradesh, India. This analysis determined the level of exposure of workers and the general public to electric and magnetic fields; it concluded that the calculated values were well below the limits recommended by international standards. However, it does not present a comparative analysis of the results with specialized software. Similarly, in [28], the comparative analysis of the finite element method and the image method is carried out with COMSOL Multiphysics and MATLAB for the 1,200 kV line Indian analysis. It evidenced that when comparing the results of the field profile between COMSOL Multiphysics and MATLAB.

The software presented above presents some limitations. The results evidenced that they are not capable of generating, displaying, and saving the outcomes associated with different calculation process in diverse formats. Such as the matrix of capacitances, linear charge densities, and instantaneous and effective variables related to the intensity of the electric field, intensity-density of the magnetic field. Additionally, there is no evidence that they allow visualizing the value of the instantaneous or effective electric or magnetic field at particular points or changing the step used to build the profile in the easement area.

This work is organized and presented in five sections including introduction. Section 2 describes the mathematical formulation (electric field and magnetic field). Section 3 presents the method that describes each of the modules and the sub-modules. In section 4, the results obtained for two case studies implemented are presented and analyzed. Finally, the section 5 establishes the general conclusions of the work.

## 2. MATHEMATICAL FORMULATION

### 2.1. The electric field strength in transmission lines

The analysis presented considers the ground like a perfectly conductive element, a completely flat field with infinite lines on the surface. To calculate the electric field intensity  $E$  generated by the transmission line, the linear charge densities  $\rho_{Lk}$  (where  $k$  is the number of conductors in the system, including the guard conductors), associated with each of the conductors and their images based on the Maxwell coefficient matrix and the supply voltages of the conductors:  $[V] = [P][\rho_{Lk}]$  [29]. Once determined the vector of linear charge densities  $[\rho_{Lk}]$ , from the matrix product between the inverse of the Maxwell coefficient matrix  $[P]$  and the vector of phase voltages of the system  $[V]$ , the electric field intensity  $E$  considering the actual conductors and their corresponding images. According to the mentioned, the vertical and horizontal components of the electric field generated by the transmission line for the single-phase case are given by (1) and (2):

$$E_{x_1} = \left( \frac{\rho L_1}{2\pi\epsilon_0} \right) \left( \frac{x-x_i}{(x-x_i)^2+(y-y_i)^2} - \frac{x-x_i}{(x-x_i)^2+(y+y_i)^2} \right) a_x \left[ \frac{V}{m} \right] \quad (1)$$

$$E_{y_1} = \left( \frac{\rho L_1}{2\pi\epsilon_0} \right) \left( \frac{y-y_i}{(x-x_i)^2+(y-y_i)^2} - \frac{y+y_i}{(x-x_i)^2+(y+y_i)^2} \right) a_y \left[ \frac{V}{m} \right] \quad (2)$$

where  $x$  and  $y$  coincide with the coordinates of the calculation point.  $x_i$  and  $y_i$  are the coordinates of the actual conductors and their images. For the three-phase case, considering the number of conductors in the system as  $k$ , the total electric field intensity will be given by (3).

$$E = \left( \sum_{i=1}^k E_{x_i} \right) a_x + \left( \sum_{i=1}^k E_{y_i} \right) a_y \left[ \frac{V}{m} \right] \quad (3)$$

## 2.2. The magnetic field strength in transmission lines

For this case, as in the previous one, the ground is considered as a perfectly conductive element, a completely flat ground with infinite lines on the ground surface, and also balanced currents for the three-phase case. From these conditions is determined the magnetic field strength  $H$  considering the actual conductors and their corresponding images that allow determining the contributions of the horizontal and vertical components; these expressions are represented for the case of a single conductor in the ground plane by (4) and (5):

$$H_{x_1} = \left( \frac{I_1}{2\pi} \right) \left( \frac{y+y_i}{(x+x_i)^2+(y+y_i)^2} - \frac{y+y_i}{(x+x_i)^2+(y-y_i)^2} \right) a_x \left[ \frac{A}{m} \right] \quad (4)$$

$$H_{y_1} = \left( \frac{I_1}{2\pi} \right) \left( \frac{x+x_i}{(x+x_i)^2+(y-y_i)^2} - \frac{x+x_i}{(x+x_i)^2+(y+y_i)^2} \right) a_y \left[ \frac{A}{m} \right] \quad (5)$$

where  $I_1$  corresponds to the current in the conductor;  $x$  and  $y$  correspond to the coordinates of the calculation point.  $x_i$ ,  $y_i$  are the coordinates of the actual conductors and their images. For the three-phase case, considering the number of conductors in the system as  $k$ , the total magnetic field strength is given through (6).

$$H = \left( \sum_{i=1}^k H_{x_i} \right) a_x + \left( \sum_{i=1}^k H_{y_i} \right) a_y \left[ \frac{A}{m} \right] \quad (6)$$

## 3. RESEARCH METHOD

Employing the MATLAB R2020b app designer tool, the CEM-LT software was developed. It consists of three main modules composed of four submodules with a graphical interface, which provide the user with graphic convenience throughout the entire process of setting of input and output variables. This software allows reducing erroneous settings through informational and emergency messages. Figure 1 presents the block diagram of the general operating process of the simulator.

### 3.1. Main menu module

This module is the first that the user sees when he opens the application. In this, the user can move through the different modules that make up the software. In the same way, it provides information about the creators of the application and enables help to guide the user in the main menu interface.

### 3.2. Electric field module

This module has four sub-modules that allow to parameterize initial variables, determine results for the electric field intensity at specific points, and generate graphs of electric field profiles of the transmission line in the requested easement area. Figure 2(a) presents the operation diagram for the electric field module. It describes the logical-mathematical process to determine the results associated with this variable. It also shows the process that the user must carry out when making use of the module.

### 3.3. Magnetic field module

This module has four sub-modules, which help the user to parameterize initial variables, determine results for the intensity of the magnetic field at specific points, and generate graphs of intensity and density profiles of the magnetic field in the entered easement zone. Figure 2(b) presents the operation diagram for the magnetic field module. It describes the logical-mathematical process to determine the results associated with this variable. It also shows the process that the user must carry out when making use of the module.

### 3.4. Three-phase system configuration sub-module

The first graphical window of the electric field and magnetic field modules represents the three-phase system configuration submodule. This sub-module parameterized the input variables, such as voltages for the electric field strength calculation and currents for the magnetic field strength estimation, the sequence of the system (positive and negative), the system frequency, the nomenclature of phase conductors and the reference phase. After the parameterization of the module, the transmission line geometry is configured.

### 3.5. Transmission line geometry submodule

Represents the second graphic window of the electric field and magnetic field modules. Enters input variables that allow parameterizing the phase and guard conductors. Allows entering the value of the geometric mean radius (GMR). It also approves entering up to 10 conductors per bundle and the separation distance between them. In addition, it allows entering the location coordinates of the conductors composing the transmission line.

### 3.6. Results submodule

The results sub-module allows generating, displaying, and exporting in different formats the results of the matrix of capacitances, linear charge densities, instantaneous electric field intensity, effective electric field intensity  $E_{rms}$  for the electric field module; spontaneous and effective magnetic field intensity and density ( $H_{rms}$ ,  $B_{rms}$ ) for the magnetic field module. Additionally, for the electric field module and the magnetic field module, the simulator allows to graph the value of the norm or the value rms in the servitude zone.

### 3.7. Graphics submodule

The graphics submodule generates, displays, and exports in different formats the metrics of the electric field and magnetic field profiles in the easement zone achieved by a transmission line. This analysis compares with international standards the limits of exposure to low-frequency electromagnetic fields generated by the power grid. Thus, the simulator presents the easement metrics for the output variables:  $E_{rms}$ ,  $H_{rms}$ ,  $B_{rms}$ , and the analysis of the vertical and horizontal components for the output variables concerning time.

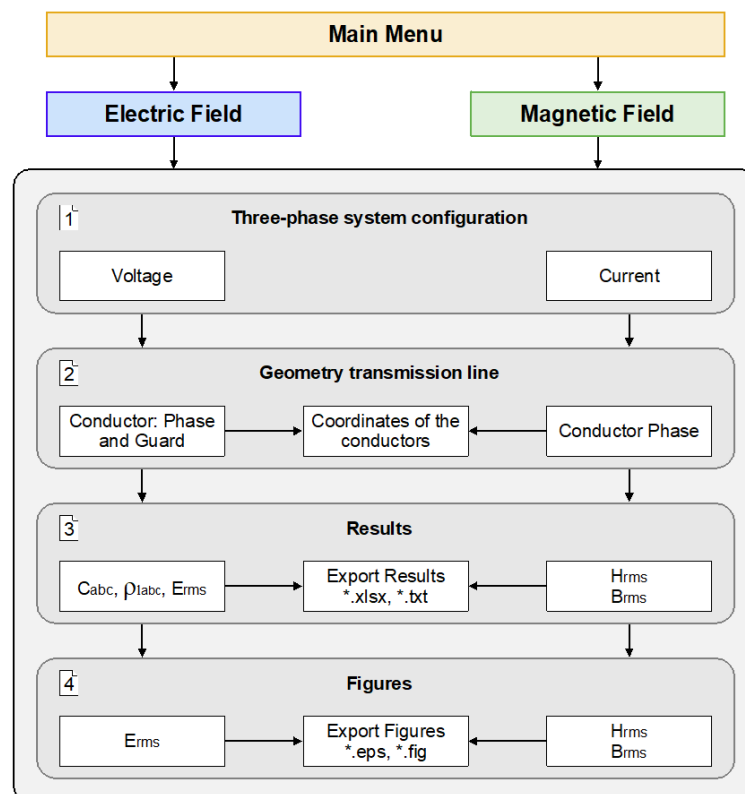


Figure 1. Description of the CEM-LT modules

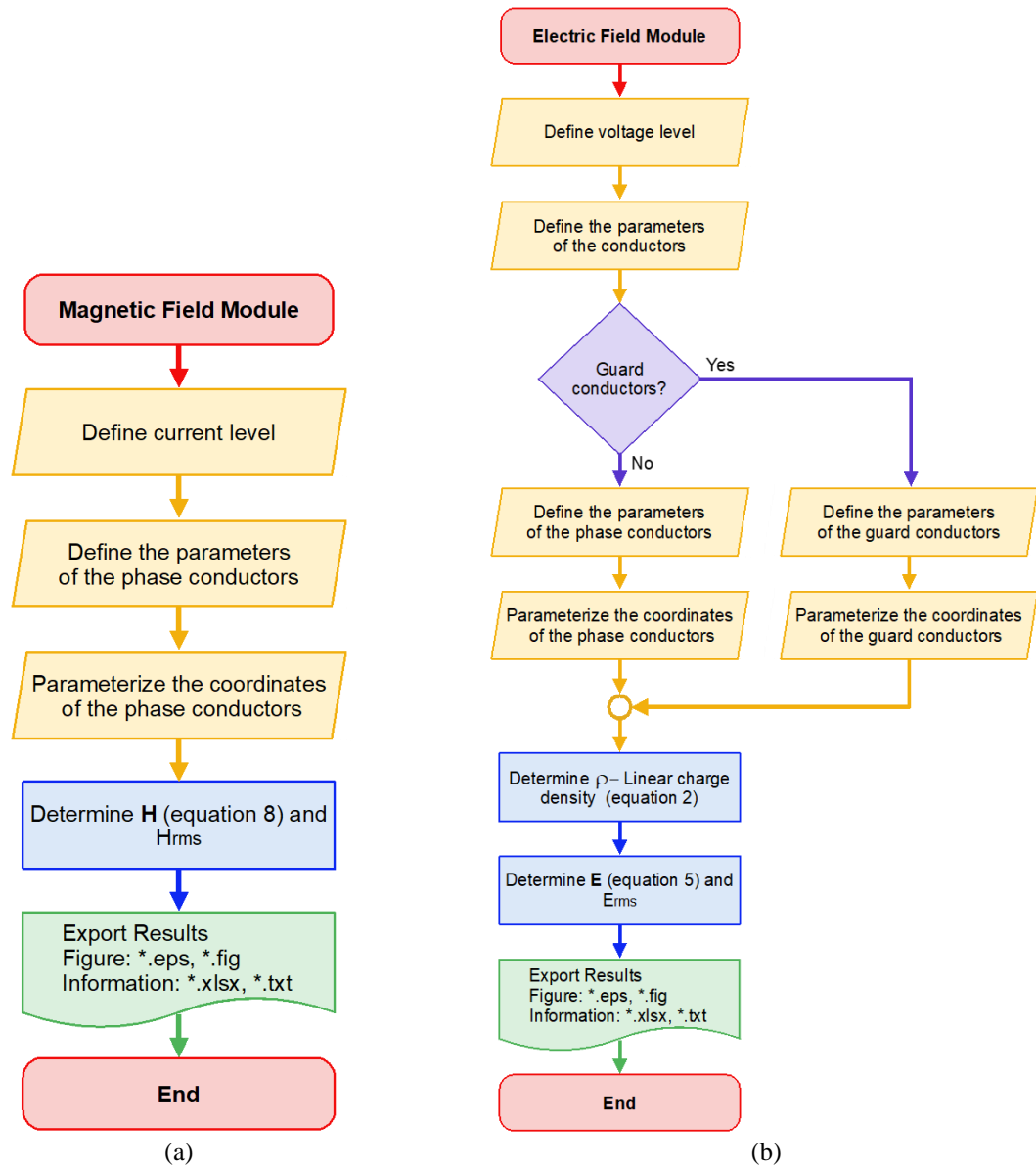


Figure 2. Flow diagram of the algorithm for (a) electric field module, and (b) magnetic field module

#### 4. RESULTS AND DISCUSSION

This section aims to evaluate the accuracy and processing time characteristics that make up the CEM-LT application. To validate the software, two case studies are presented. The comparative analysis evaluates the developed software accuracy in MATLAB App Designer CEM-LT using COMSOL Multiphysics software. In addition, using MATLAB "Profile function" application the processing times of the developed software are measured. The implementation was done on a computer with an Intel(R) Core (TM) i5-4210U CPU @1.70 GHz 2.40-6.00 GB RAM memory with Windows 10x64 bits.

##### 4.1. Case study 1

The case study to be analyzed corresponds to a 500 kV single circuit transmission line that starts from the substation of the Coca Codo Sinclair hydroelectric project to the El Inga substation in the city of Quito-Ecuador. The substation of the Coca Codo Sinclair hydroelectric project to the El Inga substation in Quito-Ecuador. Each phase of the transmission line consists of an array of four ACAR 1100 MCM 18/19 aluminum alloy conductors spaced 45 cm apart in the bundle, and two guard cables, one of bonus resistant galvanized steel and the other of OPGW fiber optic. The magnetic field study ignores the two-guard conductors. The electric field study considered guard conductors. The metal lattice structures, self-supporting cat head type, and the horizontal configuration supported the conductors [30], [31]. Figure 3 represents the

arrangement of the conductors in the transmission tower; Table 1 presents the characteristics of the phase conductors and the parameters of the transmission line San Rafael-El Inga transmission line. Figure 4 and Figure 5 show the profile of the electric field magnitude and the magnetic field density, respectively, for the horizontal configuration of the 500 kV transmission line using CEM-LT (blue plot) and COMSOL Multiphysics (red line). The simulation is presented at the height of 1 m above ground level and covers the 70 m wide easement area.

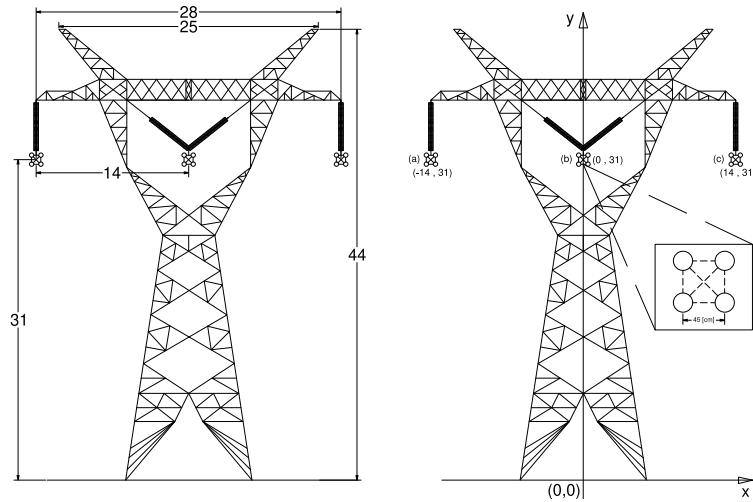


Figure 3. The geometry of a 500 kV transmission line [30]

Table 1. Characteristics and parameters of the San Rafael-El Inga line

Line configuration	Horizontal	Number of sub conductors	4
Type of line	Simple circuit	Sub Conductor spacing [cm]	45
Line r.m.s. voltage [kV]	500	Cable type and gauge Kcmil	ACAR (18/19) 1100
Maximum line current [kA]	1.8	RMG phase conductor [mm]	13.95

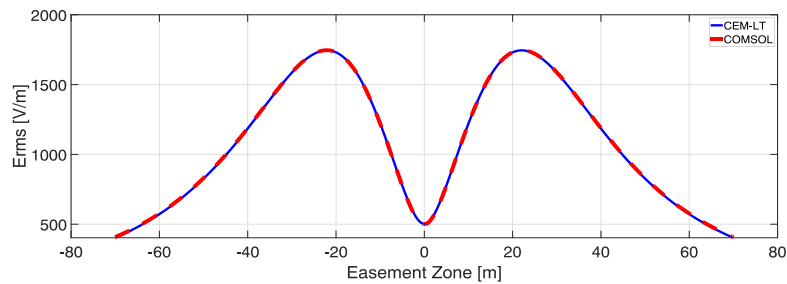


Figure 4. Active electric field profile for the horizontal configuration

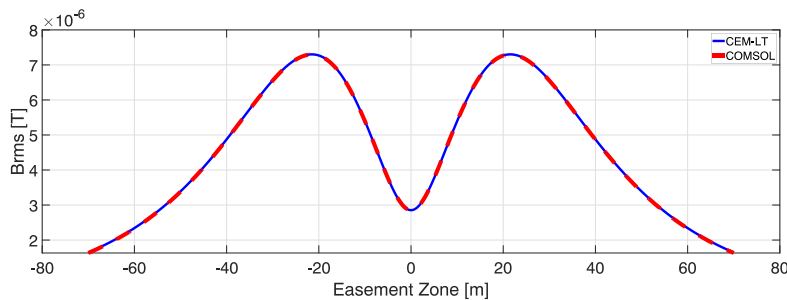


Figure 5. Active magnetic field density profile for the horizontal configuration

Electric and magnetic field distribution: when comparing the active electric field values at specific points in the easement area calculated by COMSOL Multiphysics and CEM-LT software, the percentage difference taking COMSOL Multiphysics as a reference did not exceed 1.5%. When comparing the magnitude values of effective magnetic field density at specific points in the easement area, determined by simulation in COMSOL Multiphysics and CEM-LT software, the difference taking COMSOL Multiphysics as a reference did not exceed %.

Table 2 represents the processing times for case study 1. There are determined times required by the CEM-LT software to perform the operations associated with the electric field and magnetic field calculations for two easement zones 70 m wide from the center of the line, one with steps of 0.1 m for a total of 1,401 points, and the second with strides of 0.01 m for a total of 14,001 points. Times below 1 s are evident for the estimated electric and magnetic fields in the easement zone with steps of 0.1 m. However, when making the stride much smaller (0.01 m), the processing time does not exceed 4 s.

Table 2. Characteristics and parameters of the San Rafael-El Inga line

	Steps (m)			Steps (m)	
Electric field	0.1	0.01	Magnetic field	0.1	0.01
	0.623 s	3.027 s		0.138 s	2.571 s

4.2. Case study 2

The objective in this case, aside from determining the electric and magnetic field in the easement zone for a different transmission structure, is to show one of the potentialities of the software, which consists of simulating cases where the phase location of the conductors in the transmission line is changed. In particular, it proposes an analysis of the electric and magnetic field profile in a transmission line when changing the phases under the same configuration. The analysis corresponds to a 115 kV single circuit line balanced in a negative sequence. The line phases are composed of a bundle of 3 conductors in aluminum alloy ACAR 1100 MCM 18/19, with a maximum line current of 1,414 kA. Figure 6 shows the configuration of the transmission line and the different cases that vary the location of the phases in the transmission line.

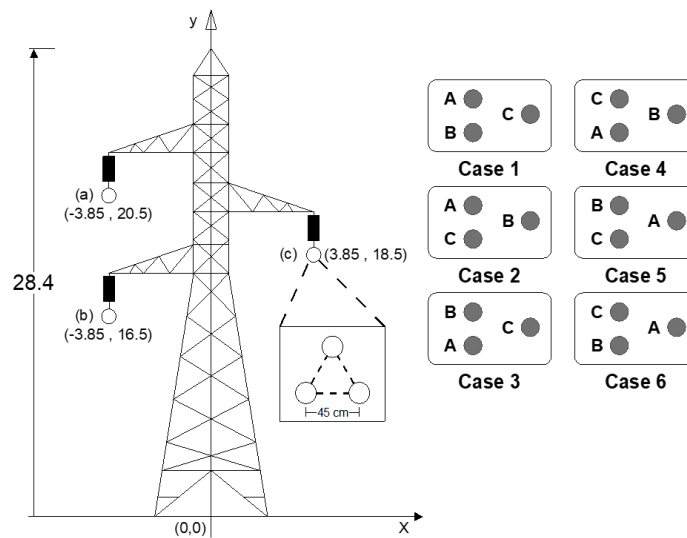


Figure 6. Geometry and phase variation of the 115 kV transmission line

Figures 7 and 8 show the behavior of the electric field and magnetic field density profiles in a 70 m wide easement zone from the center of the line, simulated in the CEM-LT software. It showed that by varying the phase sequence in the line configuration, the rms electric field in Figure 7 and magnetic field density in Figure 8 profiles over the easement zone did not show any variation. While the instantaneous values did show variations, particularly the phase angle. When comparing the values obtained in the COMSOL Multiphysics and CEM-LT software, the maximum percentage difference between the electric field data for the configuration of study case 2 is 2.4 %. In the case of the magnetic field density profile, the maximum percentage difference was 1.27 %.

Table 3 represents the processing times for case study 2. There are determined times required by the CEM-LT software to perform the operations associated with the electric field and magnetic field calculations for two easement zones 70 m wide from the center of the line, one with steps of 0.1 m, and the second with strides of 0.01 m for a total of 14,001 points. The processing time does not exceed 4 s.

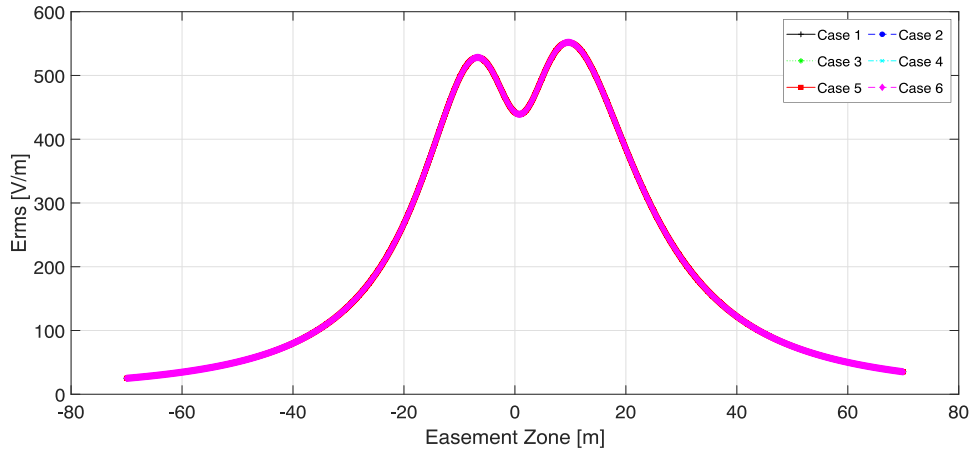


Figure 7. Electric field profile CEM-LT

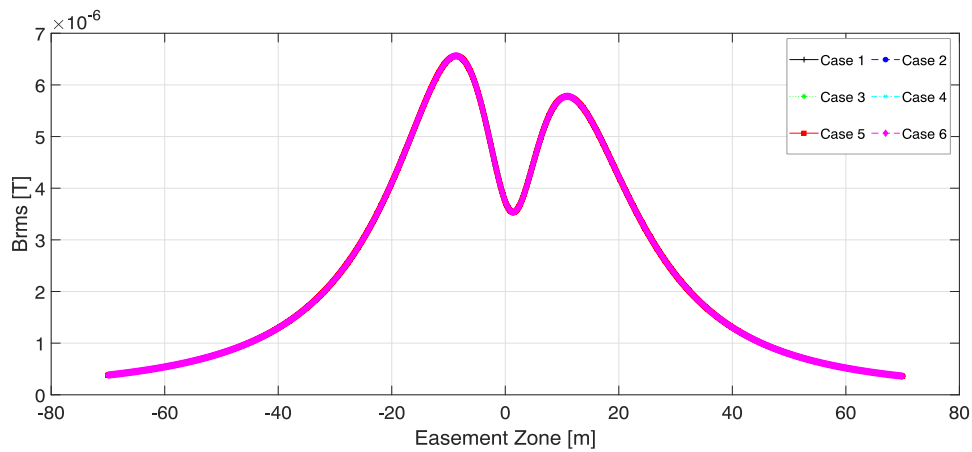


Figure 8. Profile magnetic field density CEM-LT

		Steps (m)		Steps (m)	
Electric field	0.1	0.01	Magnetic field	0.1	0.01
	0.146 s	3.078 s		0.180 s	2.580 s

**5. CONCLUSION**

This paper presents software that allows the calculation of electric field and magnetic field in overhead transmission lines as a solution to reduce the high hardware and software requirements currently used by commercial simulators based on the finite element method. The developed software showed reliable and acceptable results compared with COMSOL Multiphysics software low frequency electric and magnetic fields estimation in transmission lines. Additionally, it showed that CEM-LT offers inferior processing times with low computational load, making it ideal to be implemented in conjunction with optimization methods.

Compared to other software designed in similar simulation environments, they present some limitations. Articles do not show the visualization of variables related to the calculations as capacitance matrix, linear charge densities, and instantaneous and adequate components of the fields at particular points



of the easement zone. These calculations represent a relevant issue if the software is used as a teaching tool in undergraduate and graduate courses. It is relevant to mention that the proposed tool only requires a MATLAB compiler, which is freely available for its operation, and also includes academic aids such as manuals and a library loaded with currently standardized conductors. Additionally, the proposed tool offers a simple and intuitive interface, which allows identifying the necessary electrical parameters to be entered, thus reducing the probability of errors.




## REFERENCES

- [1] M. S. H. Al Salameh and M. A. S. Hassouna, "Arranging overhead power transmission line conductors using swarm intelligence technique to minimize electromagnetic fields," *Progress In Electromagnetics Research B*, vol. 26, pp. 213–236, 2010, doi: 10.2528/PIERB10082104.
- [2] V. Z. Manusov, P. V. Matrenin, and N. Khasanzoda, "Swarm algorithms in dynamic optimization problem of reactive power compensation units control," *International Journal of Electrical and Computer Engineering (IJECE)*, vol. 9, no. 5, pp. 3967–3974, 2019, doi: 10.11591/ijece.v9i5.pp3967-3974.
- [3] T. S. Kishore and S. K. Singal, "Optimal economic planning of power transmission lines: A review," *Renewable and Sustainable Energy Reviews*, vol. 39, pp. 949–974, Nov. 2014, doi: 10.1016/j.rser.2014.07.125.
- [4] K. A. Vyas and J. G. Jamnani, "Analysis and design optimization of 765 kV transmission line based on electric and magnetic fields for different line configurations," in *2016 IEEE 6th International Conference on Power Systems (ICPS)*, Mar. 2016, pp. 1–6, doi: 10.1109/ICPS.2016.7584136.
- [5] M. El Hajji, H. Mahmoudi, and M. Labbadi, "The electromagnetic interference caused by high voltage power lines along the electrical railway equipment," *International Journal of Electrical and Computer Engineering*, vol. 10, no. 5, pp. 4581–4591, Oct. 2020, doi: 10.11591/ijece.v10i5.pp4581-4591.
- [6] M. H. M. Sharif, N. A. M. Jamail, N. A. Othman, and M. S. Kamarudin, "Analysis of electric field and current density on XLPE insulator," *International Journal of Electrical and Computer Engineering (IJECE)*, vol. 7, no. 6, pp. 3095–3104, Dec. 2017, doi: 10.11591/ijece.v7i6.pp3095-3104.
- [7] H. M. Luqman, M. N. R. Baharom, H. Ahmad, and I. Ullah, "Planning and conducting magnetic field level measurement from overhead transmission line," *International Journal of Electrical and Computer Engineering (IJECE)*, vol. 7, no. 6, pp. 3124–3132, 2017, doi: 10.11591/ijece.v7i6.pp3124-3132.
- [8] World Health Organization, "Electromagnetic fields and public health; exposure to extremely low frequency fields," *Environmental Health Criteria*, no. 238, pp. 1–519, 2007.
- [9] T. Miah and D. Kamat, "Current understanding of the health effects of electromagnetic fields," *Pediatric Annals*, vol. 46, no. 4, pp. e172–e173, Apr. 2017, doi: 10.3928/19382359-20170316-01.
- [10] J. H. Kim, J.-K. Lee, H.-G. Kim, K.-B. Kim, and H. R. Kim, "Possible effects of radiofrequency electromagnetic field exposure on central nerve system," *Biomolecules & Therapeutics*, vol. 27, no. 3, pp. 265–275, May 2019, doi: 10.4062/biomolther.2018.152.
- [11] J.-H. Moon, "Health effects of electromagnetic fields on children," *Clinical and Experimental Pediatrics*, vol. 63, no. 11, pp. 422–428, Nov. 2020, doi: 10.3345/cep.2019.01494.
- [12] M. Soffritti *et al.*, "Life-span exposure to sinusoidal-50 Hz magnetic field and acute low-dose  $\gamma$  radiation induce carcinogenic effects in Sprague-Dawley rats," *International Journal of Radiation Biology*, vol. 92, no. 4, pp. 202–214, Apr. 2016, doi: 10.3109/09553002.2016.1144942.
- [13] K. Przystupa, "Electromagnetic pollution: Case study of energy transmission lines and radio transmission equipment," *Przegląd Elektrotechniczny*, vol. 1, no. 2, pp. 54–57, Feb. 2020, doi: 10.15199/48.2020.02.11.
- [14] A. T. Amoon *et al.*, "Proximity to overhead power lines and childhood leukaemia: an international pooled analysis," *British Journal of Cancer*, vol. 119, no. 3, pp. 364–373, Aug. 2018, doi: 10.1038/s41416-018-0097-7.
- [15] K. J. Bunch, J. Swanson, T. J. Vincent, and M. F. G. Murphy, "Epidemiological study of power lines and childhood cancer in the UK: Further analyses," *Journal of Radiological Protection*, vol. 36, no. 3, pp. 437–455, 2016, doi: 10.1088/0952-4746/36/3/437.
- [16] C. M. Crespi, J. Swanson, X. P. Vergara, and L. Kheifets, "Childhood leukemia risk in the California Power Line Study: Magnetic fields versus distance from power lines," *Environmental Research*, vol. 171, pp. 530–535, Apr. 2019, doi: 10.1016/j.envres.2019.01.022.
- [17] J. Huang *et al.*, "Association between exposure to electromagnetic fields from high voltage transmission lines and neurobehavioral function in children," *PLoS ONE*, vol. 8, no. 7, Jul. 2013, doi: 10.1371/journal.pone.0067284.
- [18] C. Sage and E. Burgio, "Electromagnetic fields, pulsed radiofrequency radiation, and epigenetics: How wireless technologies may affect childhood development," *Child Development*, vol. 89, no. 1, pp. 129–136, Jan. 2018, doi: 10.1111/cdev.12824.
- [19] L. Kheifets *et al.*, "A pooled analysis of extremely low-frequency magnetic fields and childhood brain tumors," *American Journal of Epidemiology*, vol. 172, no. 7, pp. 752–761, Oct. 2010, doi: 10.1093/aje/kwq181.
- [20] P. Gajšek, P. Ravazzani, J. Grellier, T. Samaras, J. Bakos, and G. Thuróczy, "Review of studies concerning electromagnetic field (EMF) exposure assessment in Europe: low frequency fields (50 Hz–100 kHz)," *International Journal of Environmental Research and Public Health*, vol. 13, no. 9, Sep. 2016, doi: 10.3390/ijerph13090875.
- [21] ICNIRP, "Gaps in knowledge relevant to the 'guidelines for limiting exposure to time-varying electric and magnetic fields (1 Hz–100 kHz),'", *Health Physics*, vol. 118, no. 5, pp. 533–542, May 2020, doi: 10.1097/HP.0000000000001261.
- [22] ICNIRP, "Guidelines for limiting exposure to time-varying electric and magnetic fields (1 Hz to 100 kHz)," *Health Physics*, vol. 99, no. 6, pp. 818–836, Dec. 2010, doi: 10.1097/HP.0b013e3181f06c86.
- [23] IEEE Std 644-1994, "IEEE standard procedures for measurement of power frequency electric and magnetic fields from AC power lines," *IEEE Std 644-2019 (Revision of IEEE Std 644-2008)*, pp. 1–40, 2020, doi: 10.1109/IEEESTD.2020.9068517.
- [24] K. Vyas and J. G. Jamnani, "Cost effective design of extra high voltage transmission lines for minimizing transmission congestion problems," *International Journal of Innovative Technology and Exploring Engineering*, vol. 8, no. 11, pp. 1257–1262, Sep. 2019, doi: 10.35940/ijitee.J9455.0981119.
- [25] E. Lunca, S. Ursache, and A. Salceanu, "Computation and analysis of the extremely low frequency electric and magnetic fields generated by two designs of 400 kV overhead transmission lines," *Measurement*, vol. 124, pp. 197–204, Aug. 2018, doi: 10.1016/j.measurement.2018.04.012.
- [26] C. A. F. Freitas and H. D. M. Braz, "Calculation and three-dimensional analysis of electric and magnetic fields on transmission




- lines with MATLAB®," in *2018 Simposio Brasileiro de Sistemas Elétricos (SBSE)*, May 2018, pp. 1–6, doi: 10.1109/SBSE.2018.8395810.
- [27] M. G. Unde and B. E. Kushare, "Analysis of electromagnetic fields of 1200kV UHV-AC transmission lines," in *2013 5th International Conference on Computational Intelligence and Communication Networks*, Sep. 2013, pp. 580–584, doi: 10.1109/CICN.2013.126.
- [28] M. A. Deshpande and M. A. Arora, "Magnetic field of 1200kv transmission line by FEM & MATLAB," *International Journal of Engineering and Advanced Technology*, vol. 9, no. 1, pp. 1105–1110, Oct. 2019, doi: 10.35940/ijeat.A9493.109119.
- [29] R. J. Lings, "EPRI AC transmission line reference book-200 kV and above," *Electrical Power Research Institute*, vol. Third Edit, 2005.
- [30] J. D. Ramirez, K. Cabezas, P. Jiménez, R. Canelos, and B. Escobar, "Cálculo de la distribución de voltajes en las cadenas de aisladores de una línea de transmisión de 500 kV utilizando el método de los elementos finitos," *Enfoque UTE*, vol. 11, no. 3, pp. 1–14, Jul. 2020, doi: 10.29019/enfoqueute.v11n3.619.
- [31] K. D. C. Rubio and P. Corrales, "Modelación, simulación y medición de los campos electromagnéticos en una línea de extra alto voltaje mediante el método de elementos finitos, caso de aplicación a línea de transmisión de 500 kV San Rafael-El Inga.," *Escuela Politécnica Nacional*, 2019.

## BIOGRAPHIES OF AUTHORS






**Luis Imbachi Guerrero**    was born in Bogotá D.C., Colombia. Electrical engineer from the Universidad Distrital Francisco José de Caldas. Currently, he works as an assistant in the Electricity Laboratories of the Technological Faculty of the Since 2005. His research interests include the safety of industrial systems, residential and industrial electrical design, fault analysis, and the study of electromagnetic fields in transmission lines. He can be contacted by email: [lfinbachig@correo.udistrital.edu.co](mailto:lfinbachig@correo.udistrital.edu.co).






**Fredy Jiménez Rubio**    was born in Bogotá D.C., Colombia. Electrical engineer from the Universidad Distrital Francisco José de Caldas. Currently, he works as a project engineer for medium and high voltage electrical substations in the Colombian energy sector. His research interests include automation and supervision of electrical substations, electrical design in control and protection systems, electrical networks, protection relays, power transmission lines, power transmission protection. He can be contacted at email: [fajimenezr@correo.udistrital.edu.co](mailto:fajimenezr@correo.udistrital.edu.co).



**Mario Rodríguez Barrera**    was born in Tunja, Colombia in 1974. He received his M.S. degree in electrical engineering from National University of Colombia, Bogotá, in 2000, and the Ph.D. degree in electrical engineering from Federal University of Santa Catarina, Florianópolis, Brazil in 2015. Since 2005, he has been an Assistant Professor with the Electrical Engineering Department of Universidad Distrital Francisco José de Caldas in Bogotá, Colombia. His research interests include electromagnetic fields, electromagnetic compatibility and numerical methods in electromagnetics. He can be contacted at email: [marodriguezb@udistrital.edu.co](mailto:marodriguezb@udistrital.edu.co).



**Diego Giral-Ramírez**    was born in Bogotá D.C., Colombia. He received his undergraduate academic and master's degree in Electrical Engineering. He is currently a doctor student in engineering at the Universidad Distrital Francisco José de Caldas. He is Assistant Professor at Electrical Engineering programs from Universidad Distrital Francisco José de Caldas in Colombia. His research interests include mathematical optimization, automation, and intelligent systems. He can be contacted at email: [dagiralr@udistrital.edu.co](mailto:dagiralr@udistrital.edu.co).